
A Concept-Centric Approach to Multi-Modality Learning

Yuchong Geng **Ao Tang**
School of Electrical and Computer Engineering
Cornell University
Ithaca, NY 14850
{yg534, atang}@cornell.edu

Abstract

In an effort to create a more efficient AI system, we introduce a new multi-modality learning framework that leverages a modality-agnostic concept space possessing abstract knowledge and a set of modality-specific projection models tailored to process distinct modality inputs and map them onto the concept space. Decoupled from specific modalities and their associated projection models, the concept space focuses on learning abstract knowledge that is universally applicable across modalities. Subsequently, the knowledge embedded into the concept space streamlines the learning processes of modality-specific projection models. We evaluate our framework on two popular tasks: Image-Text Matching and Visual Question Answering. Our framework achieves performance on par with benchmark models while demonstrating more efficient learning curves.

1 Introduction

Humans are capable of learning knowledge at a remarkable speed even during younger ages, which is in drastic contrast to most learning frameworks that require substantial resources to achieve human-like intelligence on specific tasks. Moreover, despite the exciting advancements from Large Language Models with multi-modality adaptations, there is hot debate over whether these models have achieved general intelligence or if they merely function via lossy compression of training corpora. We believe a concept-centric approach to multi-modality learning could be the key to not only bridging the efficiency gap but also marching towards a more natural learning process that mimics human learning.

At the center of our framework is a concept space that carries universal knowledge applicable to diverse modalities. Recent inspiring works on Concept Learning often focus on linking concepts to specific neurons (Liu et al., 2023b) and encoded embedding vectors (Kalibhat et al., 2023; Wang et al., 2023) of a model or injecting specific concepts as neurons into a model’s structure (Sheth & Kahou, 2023; Koh et al., 2020). Compared to these works, our proposed framework takes a systematic approach by organizing modality-agnostic abstract concepts in an interpretable knowledge space and establishing connections to different modalities by projecting modality-specific inputs onto the same space.

While it is common in multi-modality learning to create a shared representation space for multiple modalities (Radford et al., 2021; Li et al., 2022; Ramesh et al., 2022) or even utilize projections to align features from different modalities (Liu et al., 2023a), our shared concept space differentiates itself by possessing abstract knowledge which facilitates efficient learning and effortless incorporation of new modalities into the framework, as demonstrated in our experiments. We believe the proposed framework is a step closer to matching the capabilities of human learning, where we excel in creating a cohesive comprehension of concepts and seamlessly connecting multiple modalities, such as vision and language, to the learned knowledge.

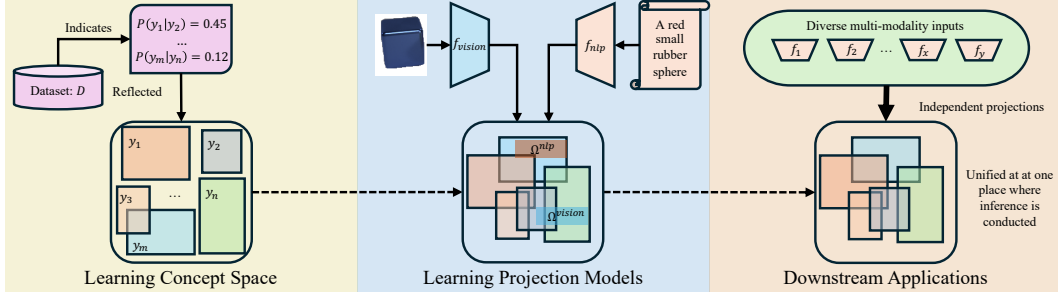


Figure 1: Overall structure of the proposed concept-centric multi-modality learning framework. A modality-agnostic concept space is trained to reflect the relations between the set of concepts \mathcal{Y} as observed in a training dataset \mathcal{D} (left). Modality-specific projection models are trained to create projections Ω for their inputs based on the inputs’ associations with concepts (middle). The modular design of the framework offers great flexibility and adaptability to a wide range of downstream tasks (right).

Specifically, as outlined in Fig. 1, the proposed multi-modality learning framework features an abstract concept space and a set of modality-specific projection models. The modality-agnostic concept space, inspired by prior works on structured embedding space (Vilnis et al., 2018; Li et al., 2018), optimally reflects real-world relations between concepts via entailment probabilities (Fig. 1 left). Probing into this concept space can also be achieved through simple queries of interested concept pairs, bringing interpretability into the learned knowledge.

Complementing the concept space, modality-specific projection models process and project distinct modality inputs onto the domain where the concept space is in (Fig. 1 middle). We call this domain the knowledge space as it hosts and bridges abstract knowledge embedded onto the concept space as well as specific knowledge extracted from material inputs. Decoupling the concept space from the projection models streamlines learning by unifying knowledge in an embedding space shared across modalities. The only restriction on the projection models is to produce consistent outputs that reside in the knowledge space, allowing them to be customized for their diverse modality inputs. This flexibility facilitates the seamless integration of different modalities, whose projection processes remain independent of each other. Naturally, the modular design of our framework extends its support to various downstream tasks, with inference processes conducted within the knowledge space (Fig. 1 right).

Contribution. Our contributions are three-fold. *First*, we propose a novel approach to multi-modality learning that centers around a concept space embedded with universally applicable knowledge. To our knowledge, this idea of a concept-focused learning scheme has rarely been explored in the field of multi-modality learning (Sec. 3). *Second*, we offer a clear motivation and justification for the proposed framework. Leveraging knowledge learned from the concept space, our framework demonstrates more efficient learning curves compared to traditional methods (Figure 2). The effectiveness of the concept space is further validated through an ablation study (Sec. 5). *Third*, we evaluate our framework’s performance on two downstream tasks. We show that the proposed framework, with a modest pretraining footprint, achieves comparable performance to benchmarks out-of-the-box without fine-tuning. (Sec. 4).

2 Related Work

Multi-Modality Learning. Vision and language modalities remain at the forefront of multi-modality learning research, with some works exploring alternative modalities like audio (Akbari et al., 2021; Shi et al., 2022). Within the vision-language area, CLIP by Radford et al. (2021) employs two modality-specific encoders to learn a joint representation through image-text matching. A subsequent work (Ramesh et al., 2022) introduces a text-to-image generation framework, using a text encoder and an image decoder for high-quality image generation from textual descriptions. Transformer-based architectures (Vaswani et al., 2017) have been widely explored for cross-modality information exchange and learning (Singh et al., 2022a; Bao et al., 2022; Kim et al., 2021a).

Beyond combining and relating modalities, research has delved into diverse areas such as multi-modality few-shot learning (Alayrac et al., 2022; Li et al., 2021) and visual-textual pattern mining

(He & Peng, 2020). Some studies propose generalized learning frameworks applicable across various modalities (Jaegle et al., 2021; Baevski et al., 2022a,b). While these frameworks showcase strong capabilities in tasks like text-to-image generation and visual language few-shot learning, our work addresses a distinct and important issue: creating a universally applicable concept space with abstract knowledge reflecting real-world observations. Baevski et al. present a versatile representation learning framework (2022b), yet it isolates modalities, impeding cross-modality interactions. In contrast, our proposed method directly combines modalities by projecting modality-specific inputs onto a unified concept space, eliminating the information barrier between them.

Concept Learning. Early approaches to Concept Learning utilize Boolean logic for defining concepts based on relationships with other concepts (Angluin, 1988) and attributes (Mitchell, 1997). Lake et al. propose a Bayesian Program Learning framework, representing concepts as probabilistic programs (2015). Nowadays, a prevalent method involves placing concepts within a structured embedding space. Marconato et al. offer a clear interpretability definition for learned concepts in an embedding space (2022). Concept learning frameworks from Mao et al. (2019) and Li et al. (2020b) place similar concepts and their corresponding visual representations close to each other. Methods from Vilnis et al. (2018) and Mei et al. (2022) emphasize entailment relationships between concepts in learned concept spaces.

In a departure from structured concept spaces, Liu et al. propose identifying "concept neurons" responsible for learning specific concepts in a deep net (2023b). While we acknowledge that some motivating works adopt a similar concept embedding strategy, our approach stands out for several reasons. The primary distinction lies in our concept space, which reflects real-world relations by providing meaningful numerical entailment probabilities that mirror those indicated by actual concepts. Furthermore, no barrier in our concept space prevents concepts belonging to different groups, such as *red* in *color* and *cube* in *shape*, from interacting with each other. Moreover, instead of being fitted to a specific modality, our concept space is designed to be abstract and modality-agnostic, which allows interactions between inputs from different modalities.

3 Method

Our proposed multi-modality learning framework consists of a modality-agnostic concept embedding space that models underlying relationships between concepts via entailment probabilities and a set of modality-specific projection models that extract representation from single-modality inputs and project them onto the domain where the concept space is in, i.e., the knowledge space.

Learning abstract knowledge in the concept space ensures generality, which makes its domain a good landing place for extracted representations from different modalities. Decoupled from the concept space and each other, modality-specific projection models can be tailored for adaptation to their unique inputs, while modality-specific knowledge stays connected after the projection.

We describe the design of the concept space in Sec. 3.1 and projection models in Sec. 3.2. Further implementation details can be found in Sec. 4.1.

3.1 Learning Concept Space

Davis et al. describe a knowledge representation as a surrogate that both carries the *thing* that exists in the real world and serves as a medium for pragmatically efficient computation (1993). Building upon their definition of a knowledge representation, we adopt an embedding space proposed by Li et al. (2018) to organize learned representations of abstract concepts. Like mental entities of specific knowledge in our brains, where we can relate concepts to each other, abstract entities in this concept space should be capable of interacting with each other, allowing reasoning inferences. In the proposed framework, we focus on entailment relations between concepts depicted by entailment probabilities to allow interactions between concepts. Contrary to latent spaces or learned ML model parameters, probing into the learned knowledge of this concept space can be easily achieved by querying the entailment probabilities of concept pairs of interest. Furthermore, our experiments demonstrate the efficiency of learning and referencing this concept space, facilitated by its compact parameter size, which qualifies it as *a medium for pragmatically efficient computation*.

Defining Concept Space. We first define a knowledge space $\mathcal{K} \subset \mathbb{R}^d$ as a d -dimensional embedding space. Let \mathcal{Y} be a set for modality-agnostic concepts. Each concept $y \in \mathcal{Y}$ is represented in \mathcal{K}

by a box embedding (the *surrogate*), defined by a pair of vectors $\Omega_y = (\omega_{min,y}, \omega_{max,y})$, where $\omega_{min,y}, \omega_{max,y} \in \mathcal{K}$ correspond to the minimum and maximum boundaries of the box in \mathcal{K} . We use $\mathcal{C} = \{\Omega_y | y \in \mathcal{Y}\} \subset \mathcal{K}$ to denote a set of box embeddings for every concepts in \mathcal{Y} and we call \mathcal{C} the concept space whose parameters are optimized to reflect real-world knowledge.

A smoothing function $m_{\text{soft}}^i(\omega) = \frac{\text{softplus}(\omega^i)}{\text{softplus}(G_{max}^i - G_{min}^i)}$ is introduced on each dimension i of \mathcal{K} so a joint probability between two disjoint concepts can still be obtained. G_{max}^i, G_{min}^i terms are the global maximum and minimum values at the i dimension among all Ω_y s in \mathcal{C} . More details of m_{soft}^i can be found in Appendix A.1. The probability of a single concept y is calculated as $P(y) = P(\Omega_y) = \prod_{i=1}^d m_{\text{soft}}^i(\omega_{max,y} - \omega_{min,y})$. The joint probability between two concepts y_1 and y_2 is calculated as $P(y_1 \cap y_2) = P(\Omega_{y_1} \cap \Omega_{y_2}) = \prod_{i=1}^d m_{\text{soft}}^i(\min(\omega_{max,y_1}, \omega_{max,y_2}) - \max(\omega_{min,y_1}, \omega_{min,y_2}))$.

Embedding Knowledge. Let \mathcal{X}_* denote a sample space of an unspecified modality marked by $*$, where each sample can be associated by a subset of modality-agnostic concepts in \mathcal{Y} . A training dataset is given as $\mathcal{D}_* = \{(x_i^*, \mathbf{y}_i)\}_{i=1}^N$, where $x_i^* \in \mathcal{X}_*$ and $\mathbf{y}_i = \{y_j | y_j \in \mathcal{Y} \text{ and } y_j \text{ describes } x_i^*\}$. This set of concepts that describe x_i^* can include both attribute concepts, like *fluffy* and *blue*, as well as category concepts, like *dog* and *sky*.

Modality-agnostic abstract knowledge can be extracted from \mathcal{D}_* by examining entailment probabilities between concepts indicated by $\{\mathbf{y}_i\}_{i=1}^N$. Specifically, the ground-truth probability of a single concept and the entailment probability of a concept pair (y_1, y_2) are calculated by $P(y) = \frac{\text{count}(y)}{\sum_{y' \in \mathcal{Y}} \text{count}(y')}$ and $P(y_1 | y_2) = \frac{\text{count}((y_1 \cap y_2))}{\text{count}(y_2)}$ as they appear in \mathcal{D}_* .

To drive the concept space to reflect real-world relationship between concepts via entailment probabilities, the objective for pretraining \mathcal{C} is naturally defined as minimizing the Kullback–Leibler divergence between predicted probabilities obtained from \mathcal{C} and true probabilities observed in \mathcal{D}_* . In addition to true concepts in \mathbf{y}_i for each data point, a set of negative concepts is sampled and added to \mathbf{y}_i . A well-organized concept space should also reflect these negative concepts’ true entailment probabilities with the original concepts. Details of this negative sampling procedure vary by specific datasets and further information is provided in Sec. 4. For each sample, we calculate an entailment probability $Q(y_1 | y_2)$ indicated by the concept space for every possible combination of concept pairs (y_1, y_2) in \mathbf{y}_i and compare them to the true entailment probabilities $P(y_1 | y_2)$. We refer readers to Appendix A for further details regarding the concept space.

3.2 Learning Projection Models

Defining Projection Models. Decoupled from the abstract concept space, each modality-specific projection model can be viewed as a mapping function $f_* : \mathcal{X}_* \rightarrow \mathcal{K}$ that generates a box representation in \mathcal{K} for each input from its modality-specific sample space \mathcal{X}_* of an unspecified modality denoted by $*$. This projection onto \mathcal{K} allows interactions between specific objects from \mathcal{X}_* and abstract concepts in \mathcal{C} . Specifically, given a modality-specific input $x_i^* \in \mathcal{X}_*$, its representation in \mathcal{K} can be obtained by $f_*(x_i^*; \theta) = \Omega_i^*$ where $\Omega_i^* \subset \mathcal{K}$ follows the same definition of $\Omega_y \in \mathcal{C}$. With this representation made available, the probability that an object is associated with a concept c can be naturally described by an entailment probability of $P(y | x_i^*) = P(\Omega_y | \Omega_i^*)$.

Adapting to Concept Space. Given f_* ’s corresponding modality training set \mathcal{D}_* , not only should the projection produced for an input x_i^* entail a single concept y , but it should also entail **all** other concepts related to x_i^* . In other words, the projection Ω_i^* for x_i^* should lie at the **intersection** of a set of concepts that can describe x_i^* . Namely, the most optimal projection for x_i^* should maximize the entailment probability of $P(\bigcap_{y_j \in \mathbf{y}_i} y_j | x_i^*)$.

To drive projection models to produce this most optimal projection, we use a combination of a binary cross-entropy loss on attribute concepts $\mathcal{Y}^{attr} \subset \mathcal{Y}$:

$$\begin{aligned} \ell_{attr}(\mathbf{y}, \Omega_*) &= \frac{1}{|\mathcal{Y}^{attr}|} \sum_{y \in \mathcal{Y}^{attr}} \mathbb{I}(y \in \mathbf{y}) [-w \cdot \log P(\Omega_y | \Omega_*)] \\ &\quad + \mathbb{I}(y \notin \mathbf{y}) [\log(1 - P(\Omega_y | \Omega_*))] \end{aligned} \quad (1)$$

(where w is a weight assigned to positive attribute concepts)

and a multi-class cross-entropy loss with SoftMax on category concepts $\mathcal{Y}^{cat} \subset \mathcal{Y}$:

$$\ell_{cat}(\mathbf{y}, \Omega_*) = -\log \frac{\exp P(\Omega_{y^{cat}} | \Omega_*)}{\sum_{y' \in \mathcal{Y}^{cat}} \exp P(\Omega_{y'} | \Omega_*)} \quad (2)$$

(where $y^{cat} \in \mathbf{y}$)

Now, given a specific modality denoted by A and its training dataset \mathcal{D}_A . The training objective for f_A is formally described as minimizing:

$$\mathcal{L}_A(\theta_A; \mathcal{D}_A) = \frac{1}{|\mathcal{D}_A|} \sum_{(x, \mathbf{y}) \in \mathcal{D}_A} \ell_{attr}(\mathbf{y}, f_A(x; \theta_A)) + \ell_{cat}(\mathbf{y}, f_A(x; \theta_A)) \quad (3)$$

While the training objective and projection outputs remain consistent across different modalities, projection models can be customized to accommodate unique modality-specific inputs, such as images or sequences of texts, bringing flexibility and versatility to the proposed framework.

3.3 Cross Modality Joint Training

To allow probabilistic analysis for cross-modality tasks, we introduce a joint training stage that encourages different projection models to produce projections that overlap with each other’s for the same object. This joint training stage is lightweight since modality-specific projection models have already been trained and adapted to a unified concept space. It requires very modest resources, with convergence occurring within a few hundred training steps, as indicated in Fig. 5 of Appendix. Subsequently, this design with demonstrated efficiency allows the effortless incorporation of new projection models into our proposed framework, mirroring humans’ ability to learn and link knowledge across modalities in a fast and efficient manner. Specifically, consider a system with two modalities, A and B , as an example. The training dataset would be denoted as $\mathcal{D}_{A \cup B} = \{(x_i^A, x_i^B, \mathbf{y}_i)\}_{i=1}^N$, and the training objective for this joint training stage is defined as:

$$\mathcal{L}_{joint}(\theta_A, \theta_B; \mathcal{D}_{A \cup B}) = \frac{1}{2|\mathcal{D}_{A \cup B}|} \sum_{(x_A, x_B, \mathbf{y}) \in \mathcal{D}_{A \cup B}} P(f_A(x_A; \theta_A) | f_B(x_B; \theta_B)) + P(f_B(x_B; \theta_B) | f_A(x_A; \theta_A)) \quad (4)$$

The overall training objective becomes a combination of modality-specific projection losses and this joint training loss. Optionally, optimization can also include parameters from \mathcal{C} , so that the abstract knowledge learned in the concept space is adjusted based on modality-specific information. Then the objective becomes $L'_{joint} = L_{joint} + \beta L_C$ where L_C denotes the KL divergence loss of the concept space.

3.4 Adapting to Downstream Tasks

With an abstract concept space and decoupled projection models, our proposed learning framework naturally accommodates various downstream tasks involving single or multiple modalities. Regardless of the specific downstream tasks, their inference process consists of two stages: creating projections and relating them to learned knowledge. This approach more closely resembles human learning than traditional black-box models. In our daily interactions with objects, we process external stimuli like vision by creating abstract mental entities for objects we see. We then comprehend these mental entities using our understanding of the world, or, in other words, our concept space (Gärdenfors, 2014). In Section 4, we use an Image-Text Matching task involving multi-modality and a Visual Question Answering task with a single-modality-focused approach to illustrate the functionality of the proposed framework.

4 Implementation and Experiments

We base our evaluation on three datasets: CLEVR (Johnson et al., 2017a), COCO (Lin et al., 2014), and GQA (Hudson & Manning, 2019) where their concepts are formed from original and supplemental annotations. Both attribute and categorical concepts are present in COCO and GQA whereas CLEVR only contains attribute concepts. More details on the datasets and preprocessing steps can be found in Appendix B. Our experiments follow the same train and validation splits as the original datasets. The proposed framework is pretrained on the train sets and tested on the validation sets.

4.1 Pretraining

Concept Space. To ensure that each concept box always has a valid set of lower boundaries smaller than its upper boundaries, we use two vectors, $(\omega_{min,y}, \omega_{\Delta,y}) = \Omega_y$, instead of $(\omega_{min}, \omega_{max})$ to represent a box in our actual experiments, where $\omega_{\Delta} \in \mathcal{K}_{\geq 0}$ is restricted to non-negative values. A box’s upper boundaries can be obtained by $\omega_{max} = \omega_{min} + \omega_{\Delta}$. We set the dimension of \mathcal{K} to 50, based on empirical experiments. Initial values for \mathcal{C} are sampled from two uniform distributions. As for the negative sampling method, in CLEVR, the only negative concept pairs come from combinations of concepts residing in the same-attribute families, such as *(red, blue)*. For COCO and GQA, negative samples are randomly selected from all concepts. The concept space is trained for two epochs for each dataset with a batch size of 256 using an AdamW optimizer (Loshchilov & Hutter, 2017) with a learning rate of 10^{-3} . The training of this concept space can be completed quickly as there are only thousands of parameters for a moderately-sized concept space.

Projection Models. In adapting our framework to the datasets featuring vision and natural language modalities, we incorporate a vision projection model f_{vision} based on a Vision Transformer encoder (Dosovitskiy et al., 2020) and a natural language projection model f_{NL} based on a BERT encoder (Devlin et al., 2018). Both models utilize their encoders’ outputs on [CLS] tokens to generate projection boxes in \mathcal{K} . The outputs e with a dimension of 768 are divided into two equal chunks, h_{min} and h_{Δ} , each with a dimension of 384. These chunks are then input into two fully connected layers to produce ω_{min} and ω_{Δ} for their respective projection boxes. To ensure ω_{Δ} is always a non-negative vector, an additional ReLU layer is applied. The complete projection process for inputs from the vision modality is outlined in Algorithm 1.

For each object i in the CLEVR dataset, its attribute prediction for a specific attribute family z (e.g., *color*) is generated by $\hat{y}_i^z = \operatorname{argmax}_{y \in z} P(\Omega_y | \Omega_i)$. For each object i in COCO and GQA, a threshold is applied to $P(\Omega_y | \Omega_i), y \in \mathcal{Y}^{attr}$ to obtain attribute predictions, and category prediction is generated by $\hat{y}_i^{cat} = \operatorname{argmax}_{y \in \mathcal{Y}^{cat}} P(\Omega_y | \Omega_i)$.

We establish a baseline by replacing the concept space with a traditional Multilayer Perceptron (MLP) at the classification head of f_{vision} . Additionally, we implement the vision-modality projection model using a ResNet model (He et al., 2015) as the backbone to showcase the flexibility of the proposed framework. Results summarized in Table 1 show that our proposed framework achieves comparable performance to traditional models while leveraging a novel concept space with interpretable learned knowledge.

Apart from featuring a concept-centric learning scheme, the proposed framework can also learn modality-specific knowledge faster by referencing learned knowledge from the modality-agnostic concept space as indicated in Fig. 2. This more natural learning process of our framework bridges the efficiency gap between traditional machine learning methods, which often demand extensive data, and human learning, which excels at adeptly and efficiently extracting modality-specific representations and associating them with mental entities of abstract knowledge. To fully evaluate the impact of this transparent, modality-agnostic concept space on the learning of modality-specific projection models, we conduct an ablation study on it in Sec. 5.

Algorithm 1 Illustration of a ViT-based projection model f_{vision} which projects vision modality inputs to the knowledge space \mathcal{K}

input modality-specific input x_{vision}
Ensure: $\omega_{\Delta}^{vision} \in \mathcal{K}_{\geq 0}, \Omega^{vision} \subset \mathcal{K}$
 $e_{vision} \leftarrow \text{ViT}(x_{vision})$
 $h_{min}^{vision}, h_{\Delta}^{vision} \leftarrow \text{split}(e_{vision})$
 $\omega_{min}^{vision} \leftarrow \text{Linear}_{min}^{vision}(h_{min}^{vision})$
 $\omega_{\Delta}^{vision} \leftarrow \text{ReLU}(\text{Linear}_{\Delta}^{vision}(h_{\Delta}^{vision}))$
output $\Omega^{vision} = (\omega_{min}^{vision}, \omega_{\Delta}^{vision})$

Backbone	Method	CLEVR	COCO		GQA	
		Accuracy	Accuracy	F1 Score	Accuracy	F1 Score
ResNet	Baseline	0.997 \pm 1.0e $^{-4}$	0.897 \pm 1.7e $^{-3}$	0.625 \pm 2.4e $^{-3}$	0.733 \pm 4.5e $^{-3}$	0.401 \pm 2.8e $^{-3}$
	f_{vision}	0.990 \pm 2.7e $^{-3}$	0.900 \pm 7.8e $^{-4}$	0.621 \pm 2.1e $^{-3}$	0.724 \pm 1.7e $^{-3}$	0.429 \pm 3.1e $^{-3}$
ViT	Baseline	0.999 \pm 3.9e $^{-5}$	0.956 \pm 2.0e $^{-3}$	0.663 \pm 1.7e $^{-3}$	0.841 \pm 2.3e $^{-3}$	0.567 \pm 1.7e $^{-3}$
	f_{vision}	0.999 \pm 4.0e $^{-5}$	0.955 \pm 1.4e $^{-3}$	0.658 \pm 2.4e $^{-3}$	0.839 \pm 3.0e $^{-3}$	0.574 \pm 1.1e $^{-3}$

Table 1: A comparison with baseline models on classification performance of vision-modality inputs. Category concepts are evaluated with accuracy (%) and attribute concepts with f1 score. 2-sigma errors over five trails of experiments are reported

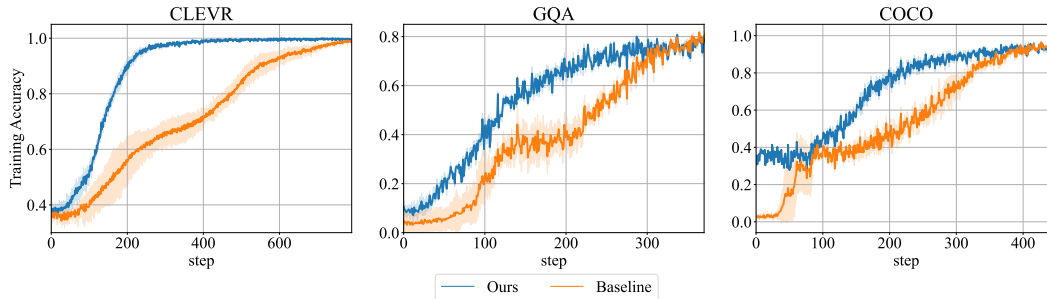


Figure 2: Learning curves of proposed projection models and baseline models. Shaded area in plots represents 2-sigma errors over five trails of experiments. During the learning process, the proposed vision-modality projection model converges faster compared to the baseline thanks to the universal concept space that already has abstract knowledge embedded in it. This faster learning process of our framework bridges the efficiency gap between traditional machine learning methods, which require a huge amount of data, and human learning that excels at extracting modality-specific representations and linking them to mental entities of abstract knowledge.

Projection models for the natural-language modality achieve highly accurate performance ($\geq 99\%$) thanks to the clearly structured description sentences. Further implementation and training details of projection models can be found in Appendix C.

Now, we focus on our proposed framework’s adaptation to two downstream tasks: Image-Text Matching involving cross-modality references and Visual Question Answering with a single-modality-focused approach.

4.2 Image-Text Matching

Image-text matching is a binary classification task on whether a natural language sentence describes an image. Our framework can naturally adopt a common approach involving creating representations for sentences and images in a shared latent space. In contrast to those works, however, our latent space is a knowledge-embedded concept space that supports efficient probing. Specifically, given an image-text pair (x_m^{vision}, x_n^{NL}) , their representations in the learned concept space \mathcal{C} are generated by $f_{vision}(x_m^{vision}) = \Omega_m^{vision}$ and $f_{NL}(x_n^{NL}) = \Omega_n^{NL}$. The probability that (x_m^{vision}, x_n^{NL}) is a positive pair can be determined by the cross entailment probability of $P(\text{matched} | (x_m^{vision}, x_n^{NL})) = \frac{1}{2} [P(\Omega_m^{vision} | \Omega_n^{NL}) + P(\Omega_n^{NL} | \Omega_m^{vision})]$. This inference process is demonstrated in Fig. 7 in Appendix.

In our experiments, we employ two methods to create negative image-text pairs: swapping whole description sentences and swapping attributes. Specifically, for the first method, we replace 50% of images’ description sentences using random sampling. For example, an original description sentence of a CLEVR object might be changed from "There is a large, metal, red cube" to "There is a *rubber, small, yellow sphere*." On the other hand, swapping attributes involves changing only a subset of attributes that describe an object, creating a more challenging image-text matching task. For instance, the same description sentence would be changed to "There is a *small*, metal, red cube."

To compare our framework’s performance, we implement other benchmark multi-modality models with applications in the Image-Text Matching task. The results are summarized in Table 2. In contrast

to those models with traditional black-box architectures, our framework displays a more efficient learning process and adopts a more transparent inference process without sacrificing its performance. Details of this experiment can be found in Appendix D.

Method	Fine-tuned?	CLEVR		COCO		GQA	
		sent.	attr.	sent.	attr.	sent.	attr.
BLIP (Li et al.)	✓	0.999	0.999	0.992	0.536	0.979	0.576
CLIP (Radford et al.)	✗	0.997	0.997	0.974	0.587	0.945	0.532
FLAVA (Singh et al.)	✓	0.998	0.998	0.992	0.505	0.980	0.536
ViLT (Kim et al.)	✓	0.994	0.994	0.985	0.515	0.965	0.555
Ours	✗	0.995	0.995	0.970	0.552	0.929	0.536

Table 2: A comparison with state-of-the-art multi-modality models on the Image-Text Matching Task. We test these models and our framework using two variants of the matching task: swapping whole sentences (sents.) and swapping attributes (attr.). Classification accuracy (%) is reported.

4.3 Visual Question Answering

Visual Question Answering (VQA) evaluates an AI system’s ability to reason about images by answering questions related to those images in a natural language format. For this task, we focus on the CLEVR dataset, whose questions are designed to include attribute identification, counting, comparison, spatial relations, and logical operations. Recently, several works (Johnson et al., 2017b; Yi et al., 2018; Mao et al., 2019; Li et al., 2020a; Mei et al., 2022) have focused on a neural-symbolic reasoning approach, using chains of symbolic programs to predict answers to these questions. Our framework’s adaptation to VQA involves using a similar set of symbolic programs, but these programs operate on the knowledge space \mathcal{K} containing interpretable concepts in \mathcal{C} instead of the high-dimensional latent spaces used by previous works.

Problem Formulation. Given an image-question pair $\{X_i^{\text{vision}}, q_i\}$ where X_i^{vision} is an original CLEVR image as shown in Fig. 6 and q_i is a natural language question such as “Are there more cubes than yellow things?”, an AI system needs to generate an answer o_i in the natural language format such as “Yes”.

Symbolic Programs. We design our symbolic programs as deterministic functions operating on \mathcal{K} . Precisely, we follow the same program definitions as proposed by Johnson et al. (2017a).

Program Generator. An LSTM model π is used to process questions into sequences of programs: $\hat{z}_i = \pi(q_i)$. We follow the same pretraining procedure used in (Johnson et al., 2017b) to train this program generator. However, as there is no fine-tuning stage in our adaptation, the parameters in π are frozen once pretraining is finished.

Object Detection and Projection. Similar to our pretraining process, we use $f_{\text{detection}}$ to obtain a set of single-object images x_i^{vision} from X_i^{vision} which are then fed into f_{vision} so their projections can be obtained. Additionally, each single object’s coordinates predicted by $f_{\text{detection}}$ are attached to its projection box so questions involving spatial relations can be inferred.

Inference Process. A correctly predicted program sequence \hat{z}_i starts with a Scene function that returns all objects in an image and ends with a program that outputs the answer o_i . Intermediate programs takes output from previous programs as inputs, which is a reoccurring process until the last function. Our concept space \mathcal{C} is mainly involved in attribute identification which follows the same rule as used when evaluating projection models’ performance in Sec. 4.1. The complete inference process is also demonstrated in Fig. 8 in Appendix.

Method	Accuracy	Fine-tuned?
SA+MLP (Johnson et al.)	73.2	✓
Dependency Tree (Cao et al.)	89.3	✓
Human (Johnson et al.)	92.6	N/A
RN (Santoro et al.)	95.5	✓
IEP (Johnson et al.)	96.9	✓
MDETR (Kamath et al.)	99.7	✓
NS-VQA (Yi et al.)	99.8	✓
Ours	96.5	✗

Table 3: A comparison between our framework’s performance and state-of-the-art models. *indicates the method does not use program annotations.

Results. We perform no fine-tuning on the concept space \mathcal{C} and vision-modality projection model f_{vision} for the VQA task. A comparison to benchmark models summarized in Table 3 shows our framework achieves performance levels on par with those fine-tuned benchmark models.

5 Ablation Study

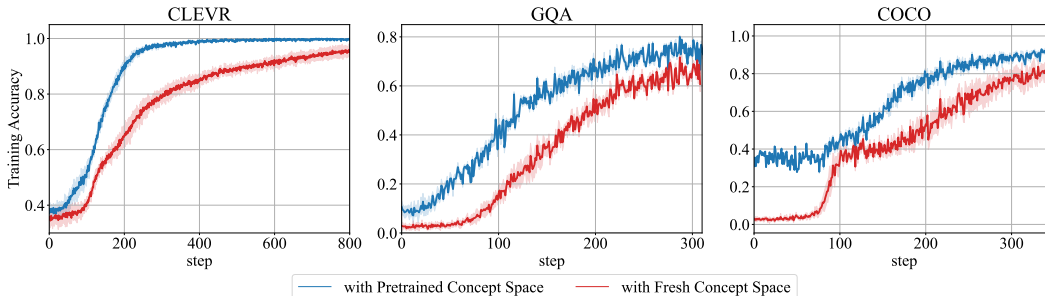


Figure 3: Ablation study on the pretrained concept space. We cut our projection models’ access to the pretrained concept space and the learning of this concept space is combined into training processes of the projection models. Shaded area in plots represents 2-sigma error over five trails of experiments. Their classification accuracy is used to compare the ablated version and the original framework.

We discover that using a pretrained concept space with learned abstract knowledge helps modality-specific projection models converge faster compared to the ones without the access. Specifically, we cut our framework’s access to the pretrained concept space \mathcal{C} . Instead, the framework is only provided with a freshly initialized concept space \mathcal{C}' and the loss function during pretraining of the vision-modality projection model is changed to $\mathcal{L}'_{\text{vision}} = \mathcal{L}_{\text{vision}} + \mathcal{L}_{\text{concept}}$. Fig. 3 shows that the original framework’s projection models can converge faster than the ablated version. Based on this evidence, we conclude that the abstract knowledge shared by the pretrained concept space streamlines the learning process of modality-specific projection models.

6 Discussion

Addressing Bias. Hidden bias learned from datasets often hinders the trustworthiness of ML systems. For example, NLP models often tend to associate the word "monarch" more with the word "male" than "female," reflected, for instance, in higher similarity scores for embeddings of "monarch" and "male." Our proposed framework facilitates effective probing into the model’s learned knowledge and offers the capacity to rectify such biases. Further demonstrations of probing into the learned concept space can be found at Appendix A.3. In the same monarch example, as training targets for concept space are simply probability distributions, bias can be easily addressed by ensuring the ground truth concept relations reflect the same entailment probability between the concept pairs of "monarch-male" and "monarch-female," which could be easily achieved from user interference.

Scalability of the Concept Space. In our experiments, the concept space is organized to reflect ground truth entailment probabilities observed in the training sets. We believe that our approach of replicating entailment probabilities from training sets can be extended to datasets with a broader array of concepts. Previous works (Vilnis et al., 2018; Li et al., 2018; Lai & Hockenmaier, 2017) have demonstrated that similar embedding spaces can accurately learn entailment probabilities for concept pairs in WordNet (WordNet). Scaling up the number of concepts introduces a challenge in generating the ground truth of entailment probabilities. We think the rich textual data available today offers a viable avenue for extracting concept relations, including entailment relations, as shown in the work by He & Peng (2020). To further verify the scalability of the concept space, we used the proposed method and fitted a concept space to the full WordNet noun entries, contributing to 10765 concepts. Measured by the KL divergence metric, the WordNet’s concept space achieves a D_{KL} of 0.1308 against ground truth. For comparison, GQA’s concept space is measured at 0.1172.

Call for Concept-Focused Datasets. In our development, we discovered a lack of high-quality datasets focused on annotating concepts in real-life images. Even with our preprocessing steps, the attribute/concept annotations in COCO and GQA are significantly noisy, partially reflected in the reduced performance of both our framework and others. We believe that potential datasets with

accurate concept annotations could not only benefit the learning of our framework but also aid in the development of more reliable and safer AI systems.

Future Works. Although our results are encouraging, we believe there is room for improvement. The current framework supports a moderate number of concepts defined by entailment relations. We envision future iterations expanding this capability to support more concepts with diverse relations. The results of the Image-Text Matching Task inspire us to explore the potential adaptation of the proposed framework to the Text-to-Image Generation task (Ramesh et al., 2022). The concept space embedded with interpretable knowledge could contribute to achieving a safer and bias-free generative process.

Conclusion. In this work, we introduce a novel multi-modality framework that centers around a concept space embedded with modality-agnostic knowledge. Our experiments show this concept-centric framework demonstrates more efficient learning curves compared to traditional architectures while maintain comparable performances on downstream tasks.

References

- Akbari, H., Yuan, L., Qian, R., Chuang, W.-H., Chang, S.-F., Cui, Y., and Gong, B. Vatt: Transformers for Multimodal Self-Supervised Learning from Raw Video, Audio and Text. *Advances in Neural Information Processing Systems*, 34:24206–24221, 2021.
- Alayrac, J.-B., Donahue, J., Luc, P., Miech, A., Barr, I., Hasson, Y., Lenc, K., Mensch, A., Millican, K., Reynolds, M., et al. Flamingo: A visual language model for few-shot learning. *Advances in Neural Information Processing Systems*, 35:23716–23736, 2022.
- Angluin, D. Queries and concept learning. *Machine learning*, 2:319–342, 1988.
- Baevski, A., Babu, A., Hsu, W.-N., and Auli, M. Efficient self-supervised learning with contextualized target representations for vision, speech and language. *ArXiv*, abs/2212.07525, 2022a.
- Baevski, A., Hsu, W.-N., Xu, Q., Babu, A., Gu, J., and Auli, M. data2vec: A General Framework for Self-supervised Learning in Speech, Vision and Language. In *International Conference on Machine Learning*, 2022b.
- Bao, H., Wang, W., Dong, L., Liu, Q., Mohammed, O. K., Aggarwal, K., Som, S., Piao, S., and Wei, F. VLMo: Unified Vision-Language Pre-Training with Mixture-of-Modality-Experts. *Advances in Neural Information Processing Systems*, 35:32897–32912, 2022.
- Cao, Q., Liang, X., Li, B., Li, G., and Lin, L. Visual question reasoning on general dependency tree. In *Proceedings of the IEEE Conference on Computer Vision and Pattern Recognition*, pp. 7249–7257, 2018.
- Davis, R., Shrobe, H., and Szolovits, P. What is a knowledge representation? *AI magazine*, 14(1): 17–17, 1993.
- Devlin, J., Chang, M.-W., Lee, K., and Toutanova, K. Bert: Pre-training of deep bidirectional transformers for language understanding. *arXiv preprint arXiv:1810.04805*, 2018.
- Dosovitskiy, A., Beyer, L., Kolesnikov, A., Weissenborn, D., Zhai, X., Unterthiner, T., Dehghani, M., Minderer, M., Heigold, G., Gelly, S., et al. An image is worth 16x16 words: Transformers for image recognition at scale. *arXiv preprint arXiv:2010.11929*, 2020.
- Gärdenfors, P. *The Geometry of Meaning: Semantics Based on Conceptual Spaces The Geometry of Meaning: Semantics Based on Conceptual Spaces*. The MIT Press, 2014.
- He, K., Zhang, X., Ren, S., and Sun, J. Deep residual learning for image recognition. *CoRR*, abs/1512.03385, 2015. URL <http://arxiv.org/abs/1512.03385>.
- He, K., Gkioxari, G., Dollár, P., and Girshick, R. Mask R-CNN. In *Proceedings of the IEEE international conference on computer vision*, pp. 2961–2969, 2017.
- He, X. and Peng, Y. Fine-grained visual-textual representation learning. *IEEE Transactions on Circuits and Systems for Video Technology*, 30:520–531, 2020.

- Hudson, D. A. and Manning, C. D. GQA: a new dataset for compositional question answering over real-world images. *CoRR*, abs/1902.09506, 2019. URL <http://arxiv.org/abs/1902.09506>.
- Jaegle, A., Gimeno, F., Brock, A., Zisserman, A., Vinyals, O., and Carreira, J. Perceiver: General Perception with Iterative Attention. In *International Conference on Machine Learning*, 2021.
- Johnson, J., Hariharan, B., Van Der Maaten, L., Fei-Fei, L., Lawrence Zitnick, C., and Girshick, R. Clevr: A Diagnostic Dataset for Compositional Language and Elementary Visual Reasoning. In *Proceedings of the IEEE conference on computer vision and pattern recognition*, pp. 2901–2910, 2017a.
- Johnson, J., Hariharan, B., Van Der Maaten, L., Hoffman, J., Fei-Fei, L., Lawrence Zitnick, C., and Girshick, R. Inferring and executing programs for visual reasoning. In *Proceedings of the IEEE international conference on computer vision*, pp. 2989–2998, 2017b.
- Kalibhat, N., Bhardwaj, S., Bruss, B., Firooz, H., Sanjabi, M., and Feizi, S. Identifying interpretable subspaces in image representations. In *Proceedings of the 40th International Conference on Machine Learning, ICML’23*. JMLR.org, 2023.
- Kamath, A., Singh, M., LeCun, Y., Misra, I., Synnaeve, G., and Carion, N. MDETR - modulated detection for end-to-end multi-modal understanding. *CoRR*, abs/2104.12763, 2021. URL <https://arxiv.org/abs/2104.12763>.
- Kim, W., Son, B., and Kim, I. ViLT: Vision-and-Language Transformer Without Convolution or Region Supervision. In *International Conference on Machine Learning*, pp. 5583–5594. PMLR, 2021a.
- Kim, W., Son, B., and Kim, I. Vilt: Vision-and-language transformer without convolution or region supervision. In *International Conference on Machine Learning*, 2021b. URL <https://api.semanticscholar.org/CorpusID:231839613>.
- Koh, P. W., Nguyen, T., Tang, Y. S., Mussmann, S., Pierson, E., Kim, B., and Liang, P. Concept bottleneck models, 2020.
- Lai, A. and Hockenmaier, J. Learning to predict denotational probabilities for modeling entailment. In Lapata, M., Blunsom, P., and Koller, A. (eds.), *Proceedings of the 15th Conference of the European Chapter of the Association for Computational Linguistics: Volume 1, Long Papers*, pp. 721–730, Valencia, Spain, April 2017. Association for Computational Linguistics. URL <https://aclanthology.org/E17-1068>.
- Lake, B. M., Salakhutdinov, R., and Tenenbaum, J. B. Human-Level Concept Learning through Probabilistic Program Induction. *Science*, 350(6266):1332–1338, 2015.
- Li, J., Li, D., Xiong, C., and Hoi, S. C. H. BLIP: bootstrapping language-image pre-training for unified vision-language understanding and generation. *CoRR*, abs/2201.12086, 2022. URL <https://arxiv.org/abs/2201.12086>.
- Li, Q., Huang, S., Hong, Y., and Zhu, S.-C. A competence-aware curriculum for visual concepts learning via question answering. In *European Conference on Computer Vision*, pp. 141–157. Springer, 2020a.
- Li, Q., Huang, S., Hong, Y., and Zhu, S.-C. A Competence-Aware Curriculum For Visual Concepts Learning via Question Answering. In *Computer Vision – ECCV 2020: 16th European Conference, Glasgow, UK, August 23–28, 2020, Proceedings, Part II*, pp. 141–157, Berlin, Heidelberg, 2020b. Springer-Verlag. ISBN 978-3-030-58535-8. doi: 10.1007/978-3-030-58536-5_9. URL https://doi.org/10.1007/978-3-030-58536-5_9.
- Li, W., Liu, X., and Bilen, H. Improving task adaptation for cross-domain few-shot learning. *CoRR*, abs/2107.00358, 2021. URL <https://arxiv.org/abs/2107.00358>.
- Li, X. L., Vilnis, L., Zhang, D., Boratko, M., and McCallum, A. Smoothing the Geometry of Probabilistic Box Embeddings. In *International Conference on Learning Representations*, 2018. URL <https://api.semanticscholar.org/CorpusID:108301524>.

- Lin, T., Maire, M., Belongie, S. J., Bourdev, L. D., Girshick, R. B., Hays, J., Perona, P., Ramanan, D., Dollár, P., and Zitnick, C. L. Microsoft COCO: common objects in context. *CoRR*, abs/1405.0312, 2014. URL <http://arxiv.org/abs/1405.0312>.
- Liu, H., Li, C., Wu, Q., and Lee, Y. J. Visual instruction tuning, 2023a.
- Liu, Z., Feng, R., Zhu, K., Zhang, Y., Zheng, K., Liu, Y., Zhao, D., Zhou, J., and Cao, Y. Cones: Concept Neurons in Diffusion Models for Customized Generation. *ArXiv*, abs/2303.05125, 2023b.
- Loshchilov, I. and Hutter, F. Decoupled weight decay regularization. *arXiv preprint arXiv:1711.05101*, 2017.
- Mao, J., Gan, C., Kohli, P., Tenenbaum, J. B., and Wu, J. The Neuro-Symbolic Concept Learner: Interpreting Scenes Words and Sentences from Natural Supervision. *ArXiv*, abs/1904.12584, 2019.
- Marconato, E., Passerini, A., and Teso, S. Glancenets: Interpretable, leak-proof concept-based models, 2022.
- Mei, L., Mao, J., Wang, Z., Gan, C., and Tenenbaum, J. B. FALCON: Fast Visual Concept Learning by Integrating Images, Linguistic descriptions, and Conceptual Relations. *ArXiv*, abs/2203.16639, 2022.
- Mitchell, T. M. *Machine Learning, International Edition*. McGraw-Hill Series in Computer Science. McGraw-Hill, 1997. ISBN 978-0-07-042807-2. URL <https://www.worldcat.org/oclc/61321007>.
- Patterson, G. and Hays, J. Coco attributes: Attributes for people, animals, and objects. In *European Conference on Computer Vision*, 2016. URL <https://api.semanticscholar.org/CorpusID:14849501>.
- Radford, A., Kim, J. W., Hallacy, C., Ramesh, A., Goh, G., Agarwal, S., Sastry, G., Askell, A., Mishkin, P., Clark, J., et al. Learning Transferable Visual Models from Natural Language Supervision. In *International conference on machine learning*, pp. 8748–8763. PMLR, 2021.
- Ramesh, A., Dhariwal, P., Nichol, A., Chu, C., and Chen, M. Hierarchical Text-Conditional Image Generation with CLIP Latents, 2022.
- Santoro, A., Raposo, D., Barrett, D. G., Malinowski, M., Pascanu, R., Battaglia, P., and Lillicrap, T. A simple neural network module for relational reasoning. *Advances in neural information processing systems*, 30, 2017.
- Sheth, I. and Kahou, S. E. Auxiliary losses for learning generalizable concept-based models. In *Thirty-seventh Conference on Neural Information Processing Systems*, 2023. URL <https://openreview.net/forum?id=jvYXln6Gzn>.
- Shi, B., Mohamed, A., and Hsu, W.-N. Learning Lip-Based Audio-Visual Speaker Embeddings with AV-HuBERT, 2022.
- Singh, A., Hu, R., Goswami, V., Couairon, G., Galuba, W., Rohrbach, M., and Kiela, D. FLAVA: A Foundational Language And Vision Alignment Model. In *Proceedings of the IEEE/CVF Conference on Computer Vision and Pattern Recognition*, pp. 15638–15650, 2022a.
- Singh, A., Hu, R., Goswami, V., Couairon, G., Galuba, W., Rohrbach, M., and Kiela, D. Flava: A foundational language and vision alignment model. In *Proceedings of the IEEE/CVF Conference on Computer Vision and Pattern Recognition*, pp. 15638–15650, 2022b.
- Vaswani, A., Shazeer, N., Parmar, N., Uszkoreit, J., Jones, L., Gomez, A. N., Kaiser, Ł., and Polosukhin, I. Attention is All You Need. *Advances in neural information processing systems*, 30, 2017.
- Vilnis, L., Li, X., Murty, S., and McCallum, A. Probabilistic embedding of knowledge graphs with box lattice measures. In *Proceedings of the 56th Annual Meeting of the Association for Computational Linguistics (Volume 1: Long Papers)*, pp. 263–272, Melbourne, Australia, July 2018. Association for Computational Linguistics. doi: 10.18653/v1/P18-1025. URL <https://aclanthology.org/P18-1025>.

Wang, Z., Gui, L., Negrea, J., and Veitch, V. Concept algebra for (score-based) text-controlled generative models. In *Thirty-seventh Conference on Neural Information Processing Systems, 2023*. URL <https://openreview.net/forum?id=SG1rCuwdsB>.

WordNet. Wordnet, a lexical database for english. URL <https://wordnet.princeton.edu/>.

Yi, K., Wu, J., Gan, C., Torralba, A., Kohli, P., and Tenenbaum, J. Neural-symbolic vqa: Disentangling reasoning from vision and language understanding. *Advances in neural information processing systems*, 31, 2018.

A Concept Space Details

A.1 Preliminary

A smoothing function for the concept space is defined as:

$$m_{\text{soft}}^i(\omega) = \frac{\text{softplus}(\omega^i)}{\text{softplus}(G_{\text{max}}^i - G_{\text{min}}^i)} \tag{5}$$

where the denominator is a normalization term with G_{max} , G_{min} being the global maximum and minimum values at i dimension. In short, this smoothing function is introduced so a valid joint probability can be calculated even if two concepts/boxes are disjoint and we refer readers to Li et al. (2018) for its complete proof.

A.2 Concept Space Training Objective

We define a KL-divergence measure between a predicted conditional probability distribution $q(y_1|y_2)$ and a target $p(y_1|y_2)$ as:

$$D_{\text{KL}}(P(y_1|y_2)||Q(y_1|y_2)) = \mathbb{E}_{(y_1,y_2) \sim P} \left[\log \frac{P(y_1|y_2)}{Q(y_1|y_2)} \right] \tag{6}$$

Let $\binom{\mathbf{y}}{2}$ denote a set of all concept pairs created from 2-combination from \mathbf{y} . The objective for training the concept space is formally described as the following:

$$\mathcal{L}_{\text{concept}}(\mathcal{C}; \mathcal{D}_*) = \frac{1}{|\mathcal{D}_*|} \sum_{(x,\mathbf{y}) \in \mathcal{D}_*} \frac{1}{2 \cdot \left| \binom{\mathbf{y}}{2} \right|} \sum_{(y_1,y_2) \in \binom{\mathbf{y}}{2}} D_{\text{KL}}(P(y_1|y_2)||Q(y_1|y_2)) + D_{\text{KL}}(1 - P(y_1|y_2)||1 - Q(y_1|y_2)) \tag{7}$$

A.3 Probing into Concept Space

Figure 4 shows an example of probing into learned knowledge of the concept space exposed to CLEVR. Benefited from such efficient probing mechanism, this concept space offers more interpretability compared to traditional latent spaces or model parameters of previous learning frameworks.

Concept 1	Concept 2	Concept Space	Ground Truth
Orange	Bus	0.043	0.043
Old	Building	0.032	0.048
Smiling	Person	0.074	0.073
White	Snow	0.910	0.974
Parked	Car	0.228	0.244
Cloudy	Sky	0.173	0.192

Table 4: Sample Queries of Concepts in GQA

Table 4 shows another example of probing learned knowledge from a concept space fitted to a dataset with a greater array of concepts. Our framework enables easy querying of targeted concept pairs, which would be computationally expensive if not infeasible in traditional latent spaces.

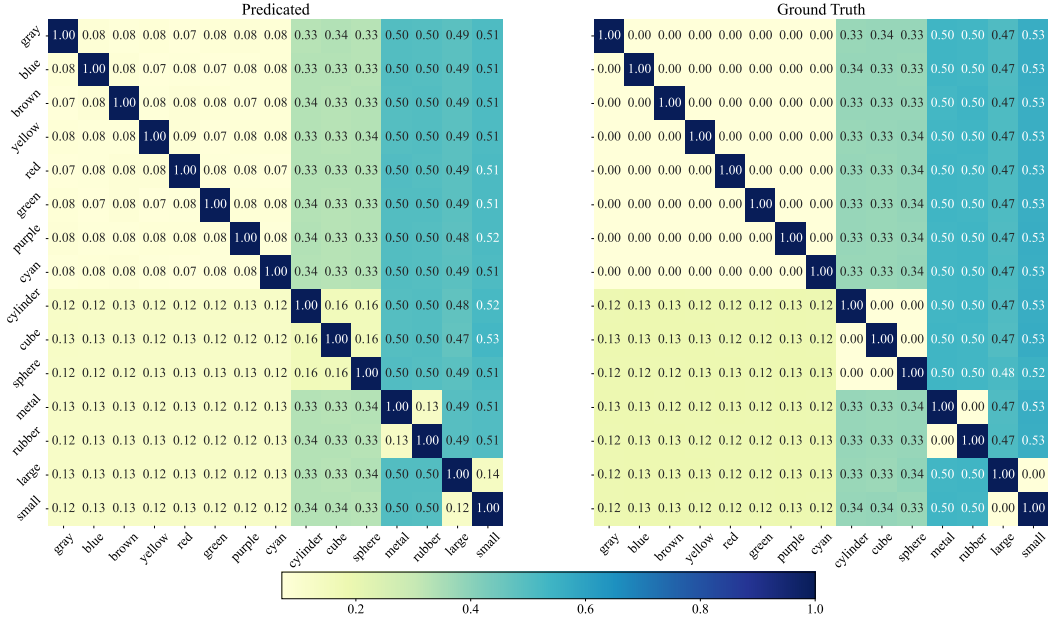


Figure 4: A comparison between the learned concept space’s understanding of the CLEVR world and the ground truth relations illustrated via entailment probabilities of concept pairs. Such comparison allows simple probing into the knowledge learned by this abstract concept space. A SoftMax function is applied on entailment probabilities of same-attribute concepts conditioned on a single concept y so $\sum_{y' \in \text{attr}_i} P(y'|y) = 1$ is satisfied.

B Evaluation Datasets and Preprocessing

We base our evaluations on three datasets:

CLEVR dataset comprises synthesized images paired with intricate questions testing a system’s visual reasoning capabilities. We choose CLEVR for evaluation because it provides a highly controlled mini-world, where concepts are easily drawn from visual objects, and relationships between concepts are clearly defined. Each CLEVR image displays a scene with a random number of objects, each described by color, shape, material, and size, which produces 15 unique values, such as blue, cube, forming attribute concepts related to specific objects.

COCO dataset exposes our framework to a knowledge world resembling the real world better than computer-generated images from CLEVR. We use attribute annotations proposed by Patterson & Hays to establish attribute concepts such as soft, cooked, and parked (2016). The original COCO classes are used as category concepts. We focus our evaluation on the top 35 frequent attributes and their associated categories to gain meaningful insights, resulting in 64 concepts.

GQA dataset is similar to COCO, providing a controlled sandbox mimicking the real world. We use the original attribute and category labels in GQA as concepts and filter out rare attributes and classes, resulting in the same amount of concepts as in COCO. Example attribute and category concepts include happy, old, gray, and boy.

Since each image in these datasets contains multiple objects, a preprocessing step is essential to isolate single objects. This isolation allows focused learning on targeted objects, reducing ambiguity. This process mirrors human learning, where attention naturally centers on a novel object while ignoring the surrounding environment Gärdenfors (2014).

Both COCO and GQA datasets already include object segmentation data. For the CLEVR dataset, we employ a MASK R-CNN model (He et al., 2017), denoted as $f_{\text{detection}}$, trained on a small amount of annotated data as an object detection model to generate segmentation. Visual object inputs are created by cropping original images to include only the objects of interest, as illustrated in Fig. 6.

In addition to object isolation, we generate a descriptive sentence for each object, introducing natural language as a new modality in the dataset. Each sentence of an object has the structure "There is

"a" followed by a sequence of values indicated by its attribute concepts in random orders to ensure diversity. Category concept values are added last to the sequence, except for CLEVR, where values from the shape attribute family are placed last for natural-sounding sentences.

C Projection Models Details

C.1 Architecture

ViT-based vision-modality projection models use a vision transformer (ViT-Base) pretrained on ImageNet-21k Dosovitskiy et al. (2020) as the backbone. The baseline MLP model is comprised of three fully-connected layers used as ViT’s classification head, with each middle layer containing 128 neurons.

ResNet-based vision-modality projection models use a ResNet model (ResNet-50) pretrained on ImageNet-21k He et al. (2015) as the backbone. Because of ResNet’s large feature vectors, the linear layer used to project feature vectors onto the concept space is expanded to a three-layer MLP, featuring two intermediate layers comprising 512 and 256 neurons, respectively. The baseline MLP model is comprised of three fully-connected layers installed after ResNet’s layers, with each middle layer containing 128 neurons.

BERT-based nlp-modality projection models use a pretrained BERT encoder (BERT-base) Devlin et al. (2018) as the backbone.

C.2 Training Details

Vision modality projection models are trained for 10 epochs with a batch size of 256 with an exception of CLEVR whose models are only trained for 1 epoch. An AdamW optimizer with a learning rate of 10^{-4} is used. Learning rate schedulers are used to achieve warm-up for first epoch and then a process of 10^{-1} linear decrease over the remaining epochs.

Natural-language modality projection models are trained for 1 epoch using the same setup and hyper-parameters as used by the vision ones.

Thresholds for attribute identification are selected based on performances from training splits. Thresholds producing the best f1 score on training sets are used in tests.

D Image-Text Matching Experiment Details

D.1 Our Framework

We follow the cross-modality joint training method and train our vision and natural language projection models for only 1 epoch with a batch size of 256 and a learning rate of 10^{-4} .

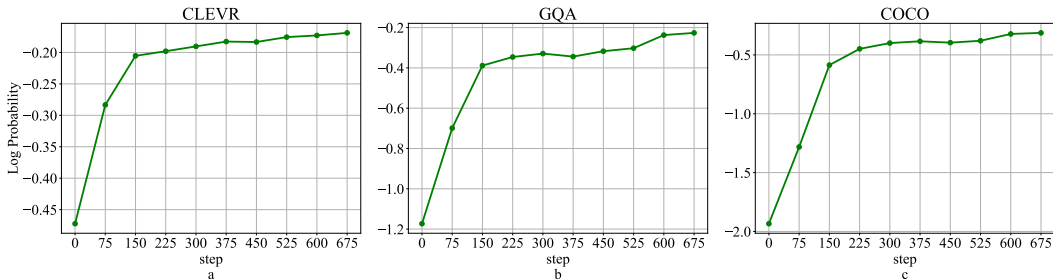


Figure 5: Cross-modality entailment probability of $P_{\text{cross}}(x_i^{\text{vision}}, x_i^{\text{NL}}) = 0.5 \cdot P(\Omega_i^{\text{vision}} | \Omega_i^{\text{NL}}) + 0.5 \cdot P(\Omega_i^{\text{NL}} | \Omega_i^{\text{vision}})$ over joint training steps. It can be observed that projection models of vision modality f_{vision} and natural language modality f_{NL} can quickly learn to produce overlapping projections for the same object in the concept space. Such quick convergence allows easy incorporation of new modalities/modalities into the proposed learning system. This joint training takes significantly less time and uses fewer GPU resources than the following BLIP and CLIP models.

Figure 5 illustrates the fast convergence of the proposed projection models on learning to produce overlapping representations of the same objects in the transparent concept space. This joint training also takes significantly less time and uses fewer GPU resources than the following BLIP and CLIP models.

D.2 BLIP

We follow the training method as stated in Li et al. (2022) and fine-tune the pretrained BLIP model directly on the Image-Text Matching task (swapping-sentence split) using both the image-text contrastive loss and a task-specific image-text matching loss produced by the image-text matching classification head in BLIP. We use a greater batch size of 512 as the calculation of image-text contrastive loss requires a large number of samples.

D.3 CLIP

We follow the training method as stated in Radford et al. (2021) and adapt the pretrained CLIP model to the general three datasets using the symmetric loss that favors larger similarity scores between positive image-text pairs and smaller scores for negative ones. We use a batch size of 512 as in BLIP during pretraining. Similar to our framework, CLIP model is not directly trained on the Image-Text Matching task.

D.4 ViLT

Similar to BLIP, we follow the training method as stated in Kim et al. (2021b) and fine-tune the pretrained ViLT model directly on Image-Text Matching task (swapping-sentence split) using a binary cross-entropy loss on the matching classification head.

D.5 FLAVA

We use the same procedures as used in ViLT to fine-tune a pretrained FLAVA model on the data domains appeared.

E Computation Resources

We run our experiments on a virtual machine (VM) hosted by Microsoft’s Azure. This VM has four NVIDIA A100 PCIe GPUs with 320 GB of total memory.

F Additional Figures

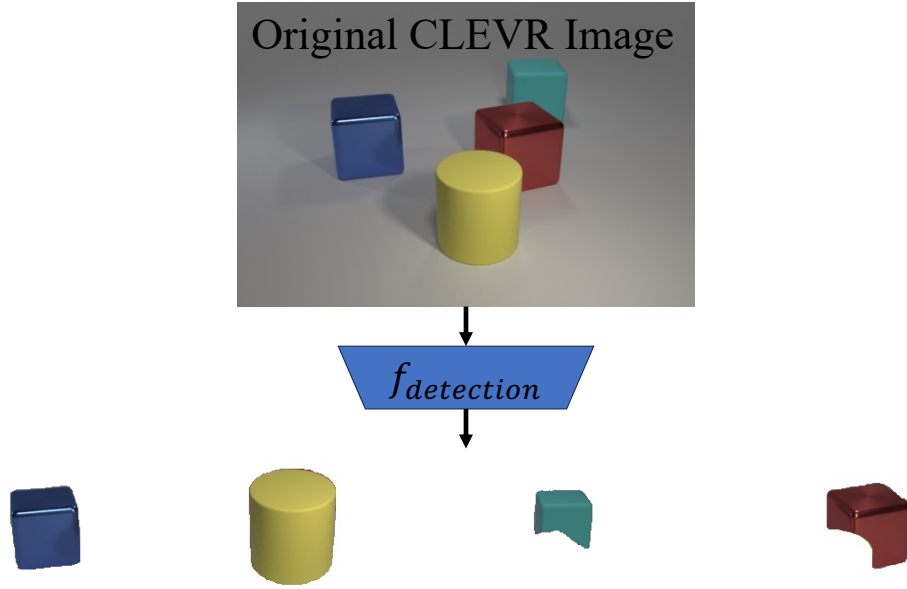


Figure 6: The segmentation masks generated by $f_{\text{detection}}$ are applied to the original CLEVR images to isolate each object from its surroundings environment. This preprocessing step enables our proposed framework to replicate the way we, as humans, naturally focus our attention on novel objects during the learning process.

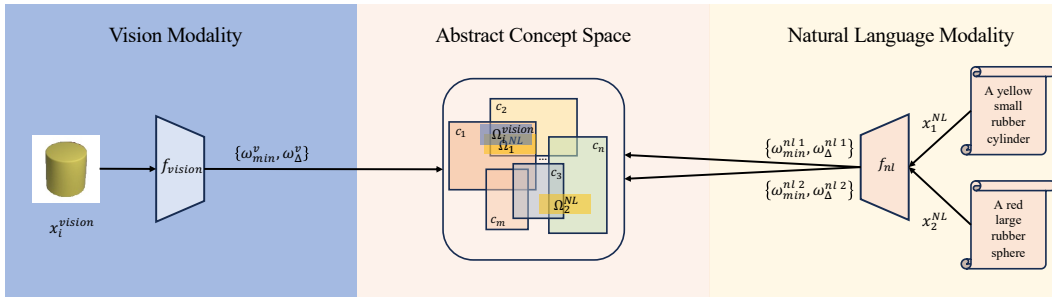


Figure 7: Application of the proposed framework on the Image-text matching task. An image x_i^{vision} of a yellow, small rubber cylinder and two description sentences $x_1^{\text{NL}}, x_2^{\text{NL}}$ are processed by their modality-specific models f_{vision} and f_{NL} which project modality-specific inputs onto a learned abstract concept space \mathcal{C} . We use the cross-entailment probability between projections of an image and a sentence to determine if they form a positive pair. While creating representations of images and sentences in a shared latent space is a common approach for the image-text matching task, our shared representation space is a knowledge-embedded concept space offering interpretability, which is in drastic contrast to the commonly used latent space with black-box structure.

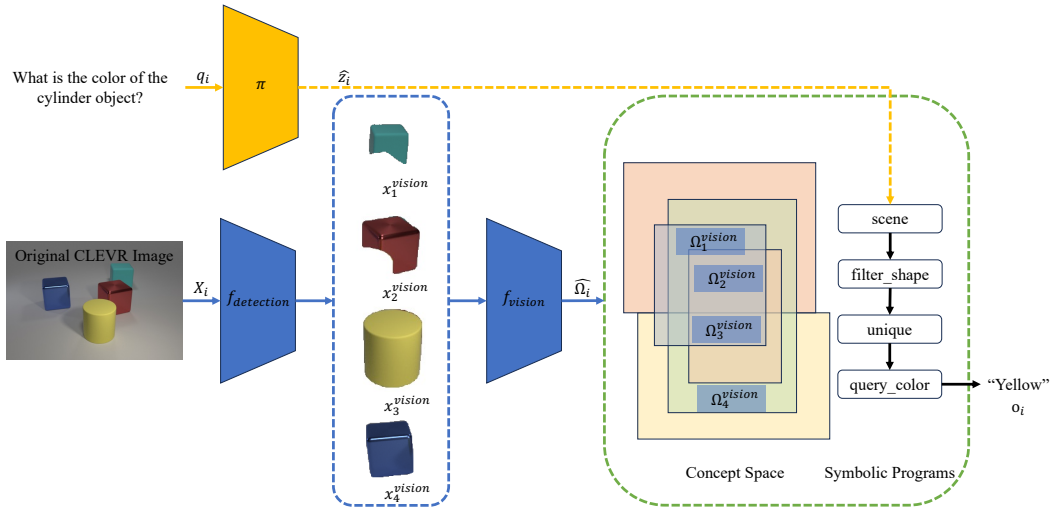


Figure 8: Application of the proposed framework to Visual Question Answering task. We reuse the object detection model $f_{detection}$ from the pretraining stage, which extracts a set of single objects x_i from an original CLEVR image X_i . The vision-modality projection model f_{vision} then projects x_i onto the \mathcal{K} . A program generator π is used to predict a sequence of symbolic programs \hat{z}_i based on an input question q_i in natural language format. Programs in \hat{z}_i operate on the concept space and produce an answer o_i to q_i .